EurJOC
European Journal of Organic Chemistry

A Journal of
ChemPubSoc Europe

Accepted Article

Title: Facile access to 12-membered macrocyclic ligand PCTA and novel derivatives including carboxylate, amide and phosphinate ligating functionalities.

Authors: Claude Picard, Morgane Enel, Nadine Leygue, Nathalie Saffon, and Chantal Galaup

To be cited as: *Eur. J. Org. Chem.* 10.1002/ejoc.201800066

Link to VoR: http://dx.doi.org/10.1002/ejoc.201800066

Supported by
ACES Asian Chemical Editorial Society

WILEY-VCH

Facile access to 12-membered macrocyclic ligand PCTA and novel derivatives including carboxylate, amide and phosphinate ligating functionalities.

Morgane Enel,[a,b] Nadine Leygue,[a,b] Nathalie Saffon,[c] Chantal Galaup,*[a,b] and Claude Picard*[a,b]

Keywords: Macrocyclic ligands – template synthesis - lanthanides

Abstract

We describe a convenient synthetic pathway for the access of the 12-membered PCTA macrocycle, a polyaminocarboxylate ligand whose M^{2+} and M^{3+} complexes are commonly associated with applications in biomedical diagnostic and radiotherapy. The synthetic pathway is based on the use of a linear tri-*N*-alkylated triamine synthon incorporating masked acetate arms and an efficient sodium template ion effect for the crucial macrocyclization step (87 % macrocyclization yield). This approach was then successfully applied to the access of three new PCTA[12] derivatives containing either a 4-pyridol unit either amide or phosphinate coordinating functions in the central side arm. In all cases macrocyclization reactions are controlled by a sodium template ion effect and display macrocyclization yields in the range 60 – 75 %. The luminescence or relaxometric properties behaviour of Eu(III), Tb(III) or Gd(III) complexes derived from mixed coordinating arms PCTA derivatives are also investigated, making these complexes as possible alternative candidates for PCTA[12]-Ln(III) complexes.

[a]*CNRS; Laboratoire de Synthèse et Physico-Chimie de Molécules d'Intérêt Biologique, SPCMIB, UMR-5068; 118 Route de Narbonne, F-31062 Toulouse cedex 9, France*
E-mail : picard@chimie.ups-tlse.fr galaup@chimie.ups-tlse.fr
http://spcmib.univ-tlse3.fr
[b]*Université de Toulouse; UPS; Laboratoire de Synthèse et Physico-Chimie de Molécules d'Intérêt Biologique, SPCMIB; 118 route de Narbonne, F-31062 Toulouse cedex 9, France*
[C] *Institut de Chimie de Toulouse (FR 2599), 118 Route de Narbonne, F-31062 Toulouse cedex 9, France*

Supporting information and ORCID(s) from the authors(s) for this article are available on the WWW under https://

Introduction

Polyazamacrocyclic ligands continue to receive considerable attention due to the widespread utility of their metal complexes. In particular, metal complexes derived from acetate functionalized polyaza macrocycles are commonly associated with applications in the general area of biomedical imaging and radiotherapy. In these fields, most of the investigated macrocyclic ligands are built on a limited number of coordinating core structures, such as DOTA (1,4,7,10-tetraazacyclododecane-1,4,7,10-tetraacetic acid) or NOTA (1,4,7-triazacyclononane-1,4,7-triacetate).[1] The popularity of these chelators is such that several precursors are now marketed. PCTA[12] (3,6,9,15-tetraazabicyclo[9.3.1]pentadeca-1(15),11,13-triene-3,6,9,-triacetic acid) is another noticeable example of this family of macrocyclic ligands. It was described for the first time by Stetter *et al.*.[2] More recently, it was assessed as an efficient $M^{2+/3+}$ chelator in various metal complexes (Figure 1).

Indeed, this aminocarboxylic acid derivative of Pyclen is known to form very stable M^{2+} / M^{3+} chelates in aqueous solutions (log K_{CuL} = 18.79, log K_{GdL} = 20.39, log K_{InL} = 24.7) and its complexes display promising properties in the field of diagnostic imaging.[3] The initial use of PCTA involved the gadolinium ion and was dedicated to magnetic resonance imaging (MRI).[4] Due to the presence of two water molecules in the first coordination sphere of the metal, Gd-PCTA chelate has higher water relaxivity (r_1^{310K} = 5.4 s^{-1} mM^{-1} at 20 MHz) than other clinically approved magnetic resonance imaging contrast agents (r_1^{310K} = 3.5 – 4.8 s^{-1} mM^{-1}).[5] Other lanthanide complexes, Eu-PCTA and Tb-PCTA, are characterized by the presence of an antenna/sensitizer effect of the pyridine chromophore and act as long-lifetime luminophores compatible with the use of time resolved luminescence technique.[6] More recently, PCTA was investigated with two β^+ emitters used for PET imaging, ^{64}Cu and ^{68}Ga, and these complexes displayed much faster radiolabeling kinetics at room temperature than DOTA.[7] PCTA and its derivatives have also been successfully used with other radiometals such as ^{111}In, a γ emitter used for SPECT imaging, as well as ^{90}Y and ^{177}Lu, two β^- emitters used for targeted radiotherapy.[8,9] These data show that PCTA[12] has a significant impact on all major imaging modalities based on metallic complexes, thus making it an additional tool of value to traditional ligands such as DOTA or NOTA.

Since the pioneering work of Stetter *et al.*,[2] thirty-five years ago, the access to PCTA[12] and its derivatives is only reported using on the Richman-Atkins methodology which affords high yields in the crucial macrocyclization step without high dilution conditions.[10] In our

earlier works, we developed a new friendly synthetic methodology which allows the preparation of 15-21 membered macrocyclic chelators derived from tri- or tetra-aminoacetate moieties and a (poly)pyridine intracyclic unit in good yields.[11] In this report, we wish to demonstrate that this synthetic methodology is also very efficient to synthesize 12-membered PCTA ligand and provides a facile access to novel PCTA derivatives containing either a 4-pyridol unit either amide or phosphinate functions in the central side arm (Figure 1).

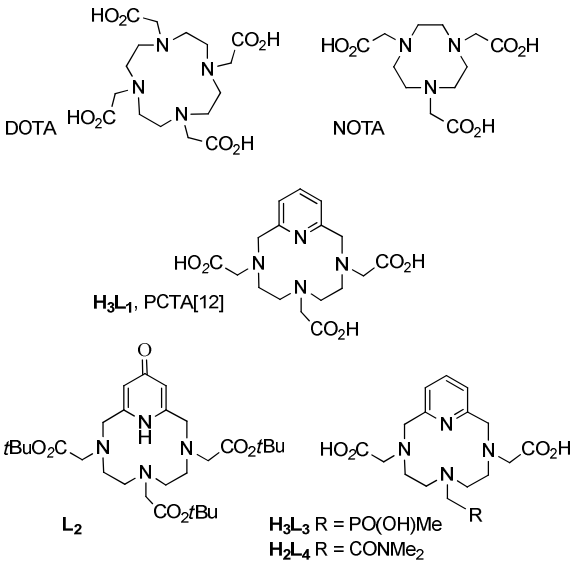

Figure 1. Structure of DOTA and NOTA ligands and PCTA[12] ligands studied in this work

Results and discussion

Currently, the route for the synthesis of PCTA is based on the preparation of Pyclen, a cyclen derivative incorporating a diethylenetriamine backbone and an intracyclic pyridine unit. (Scheme 1, route A). The access of this tetraazamacrocycle is based on the classical and time-tested Richman-Atkins macrocyclization methodology which requires the use of diethylenetriamine bearing arylsulfonamide (tosyl or nosyl) groups. In the crucial macrocyclization step, these bulky protecting groups are expected to restrict the rotational freedom of the open-chain intermediate and to shield it from intermolecular processes, promoting the cyclization reaction.[12] Although this methodology leads to high macrocyclisation yield for *N*,*N*',*N*''-trinosyl or tritosyl Pyclen derivative (76 and 94%, respectively), the three/four-step overall yield for the synthesis of PCTA[12] following this strategy is modest (27 or 36%).[13] This is a consequence of the two postmacrocyclization

steps yields: firstly, the cleavage of arylsulfonyl groups, and secondly, the per *N*-carboxyalkylation reaction, a tricky step which may require optimization of reaction conditions. However, this strategy allows easy variations in the nature of the pendant coordinating arms (amide, phosphonic acid,…).

In our strategy (Scheme 1, route B), the key macrocyclization step involves a diethylenetriamine derivative incorporating three masked acetate arms as *tert*-butyl ester and two terminal secondary amine groups. So only a single simple reaction (deprotection of ester functions) has to be conducted from the macrocyclic material. Besides, the presence of coordinating atoms in this triamine may control the formation of the 12-membered ring by a "metal-template" ion effect, thus avoiding the use of high dilution technique in the macrocyclization step. This approach allows variation on the pyridine unit without the reengineering of the whole macrocyclic molecule.

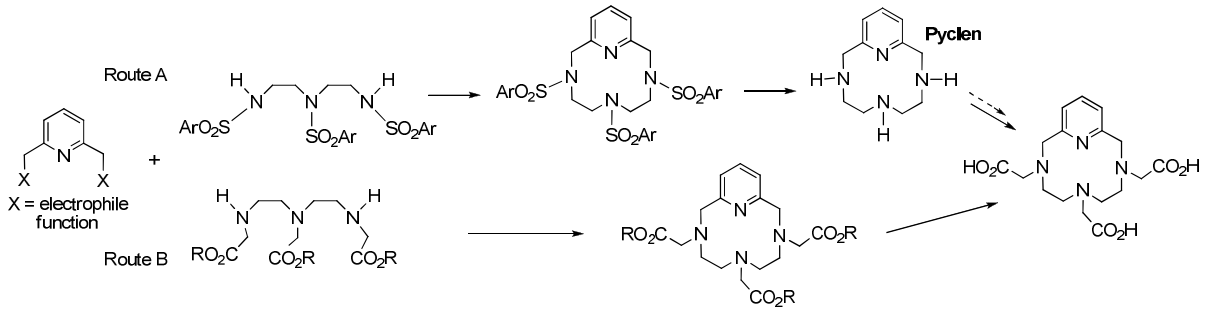

Scheme 1. General methodologies for the synthesis of PCTA[12]

In route B, the key triamine bearing *tert*-butyl ester groups may be prepared according two independent synthetic pathways as depicted in Scheme 2. Our previously reported synthetic pathway involves diethylenetriamine as starting material and affords the desired compound in two steps and 74% overall yield.[14] Briefly, reaction of diethylenetriamine with benzaldehyde and further reductive amination provided the *N*,*N*″-benzyl derivative **2**. Trialkylation of **2** with *tert*-butyl bromoacetate provided the targeted compound **6**. In the present work, we have investigated an alternative synthetic pathway in a three-step sequence starting from commercially available *N*-benzyl ethanolamine **3.** After *N*-alkylation of **3** with *tert*-butyl bromoacetate in the presence of an inorganic base (Na_2CO_3 or K_2CO_3), the hydroxyl group of **4** was then replaced by the bromine group with the NBS/PPh_3 system, using standard procedure. Reacting bromide **5** in a 2 fold excess with glycine *tert*-butyl ester in CH_3CN at

reflux and in the presence of K_2CO_3 afforded triamine compound **6** in 82% yield after purification by column chromatography. This three-step sequence affords **6** in a slightly lower overall yield (70% vs. 74%) but allows to introduce two different coordinating groups within the diethylenetriamine backbone (vide infra). Debenzylation of **6** was readily achieved in a quantitative yield by catalytic hydrogenation at room temperature under hydrogen pressure (6 bars), in methanol and using Pd/C (10 wt %) as catalyst. With these experimental conditions of hydrogenolysis, we did not observe any cleavage of the diethylenetriamine backbone as reported by Price *et al.* that use a Pd/C (5 wt %) / glacial acetic acid protocol.[15]

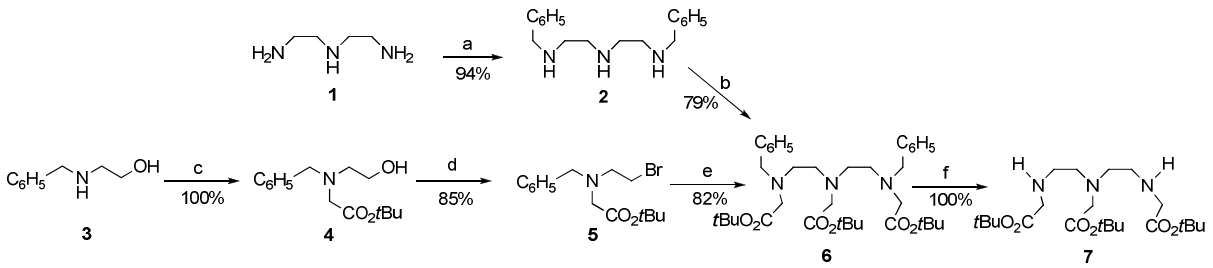

Scheme 2. Synthesis of triamine **7**. Reagents and conditions: (a) (i) C_6H_5CHO, EtOH, 50 °C, 2h; (ii) $NaBH_4$, EtOH, 50 °C, 2h, then rt, 15h; (iii) HCl (aq, 37 %). (b) $BrCH_2CO_2tBu$, DIPEA, DMF, rt, 48h. (c) $BrCH_2CO_2tBu$, K_2CO_3, CH_3CN, rt, 24h. (d) *N*-bromosuccinimide, PPh_3, CH_2Cl_2, rt 16h. (e) $NH_2CH_2CO_2tBu$ Hydrochloride salt, K_2CO_3, CH_3CN, reflux, 24h. (f) Pd/C (10%), H_2 gas (6 bars), MeOH, rt, 12h.

In addition, methyl ester was tentatively used as protection for the acetic acid chains in the key tri-substituted diethylenetriamine core (Scheme 3, compound **13**). The alkylation of *N*-benzyl ethanolamine with methyl bromoacetate in the presence of K_2CO_3 as a base and in CH_3CN at room temperature provided exclusively the lactonization product, 4-benzyl-morpholin-2-one **8**. This result was not unexpected because this side product was also observed for alkylation of **3** with benzylbromoacetate.[16] Consequently, a set of general conditions (solvent, base) was established and the main facets are gathered in Table 1. The presence of *N*,*N*-diisopropylethylamine (DIPEA) as base and DMF as solvent gave the best results, with the exclusive formation of the targeted product **9** as determined by ^1H NMR analyse of the crude reaction mixture. Attempted purification by chromatography led to a mixture of alcohol **9** and lactone **8**, as a result of silica-mediated cyclization. However, the crude material was of sufficient purity for further derivatization of the alcohol function of **9** into bromide by using the NBS/PPh_3 protocol, with a yield of 70% over the two steps. The dialkylation of glycine methyl ester by bromide **10** was carried out in DMF and in the

presence of DIPEA and provided the desired product **11** in low yield (28%), due to the extensive formation of a side product. During the reaction, intramolecular attack of the secondary amine issued from the partially alkylated reaction intermediate on methyl ester bond led to cyclization with the formation of piperazin-2-one derivative **12**. Owing to this side reaction, debenzylation of **11** by hydrogenolysis was not successfully met, leading to a complex, difficult to purify, mixture.

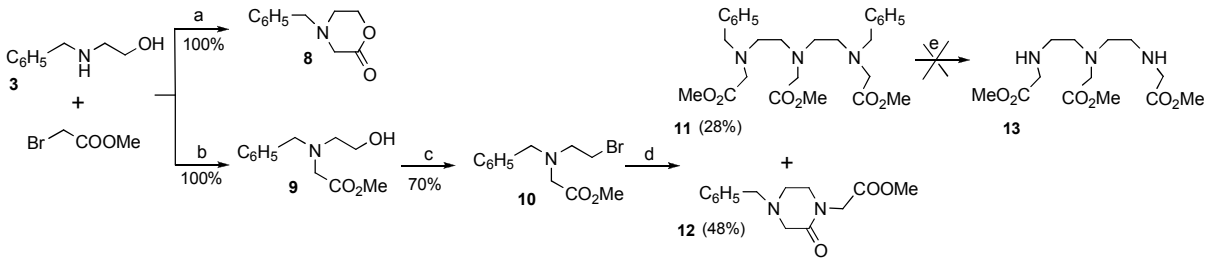

Scheme 3. Synthesis of triamine **11**. Reagents and conditions: (a) $BrCH_2CO_2Me$, K_2CO_3, CH_3CN, rt, 24h. (b) $BrCH_2CO_2Me$, DIPEA, DMF, rt, 24h. (c) *N*-bromosuccinimide, PPh_3, CH_2Cl_2, rt 16h. (d) $NH_2CH_2CO_2Me$, DIPEA, DMF, rt, 16h. (e) Pd/C (10%), H_2 gas (6 bars), MeOH, rt, 12h.

Table 1. Screening of bases and solvents[a]

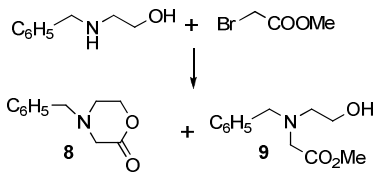

Base	Solvent	Compound **8** (%)[b]	Compound **9** (%)[b]
K_2CO_3	CH_3CN	100	0
K_2CO_3	DMF	87	13
Et_3N	CH_3CN	100	0
Et_3N	DMF	32	68
DIPEA	CH_3CN	16	86
DIPEA	DMF	0	100

[a] Reactions were carried out for 24 h at room temperature with equimolar reagents and base. [b] Percentages obtained from ^1H NMR spectra (300 MHz, $CDCl_3$) of the crude reaction mixtures. No starting material was observed in the crude reaction mixture.

Consequently, the macrocyclization reaction was attempted between *tert*-butyl acetate functionalized triamine **7** and 2,6-dibromo pyridine. This reaction was carried out under a batchwise procedure (reactants concentration: 2×10^{-3} M) and under heterogeneous

conditions in refluxing acetonitrile (48 h) with sodium carbonate as a base (Scheme 4). ^{1}H, ^{13}C NMR and MS analyses of the crude reaction product evidenced the presence of a major species, characterized as the sodium monomeric complex **14**·Na. Purification by column chromatography led to the isolation of a mixture of **14**·Na and free ligand as a result of alumina-mediated dissociation. This could be expected because of the soft character of *N*-donor atoms towards alkali metal cations. Finally, treatment of this mixture with saturated EDTA aqueous solution cleanly afforded the free ligand **14** in 87% isolated yield. Besides, treatment of free ligand **14** by Na_2CO_3 in CH_3CN at reflux afforded quantitatively **14**·Na complex. It can also be noticed that the macrocyclization reaction with dibromo derivative took place within 2 h under microwave irradiation (300 W, 90°C), affording isolated **14** in 77% yield. It is worth noting that **14** and **14**·Na species can be readily distinguished by ^{1}H NMR spectroscopy, reflecting a fluxional macrocyclic system for the free ligand 14 and a more rigid system for **14**·Na because of the presence of sodium ion.(Figure 2). On the other hand, Complexation by Na^+ was also accompanied by a reduction in the frequency of the carbonyl infrared band (8 cm^{-1}), suggesting that the ester groups are involved in complexation. In order to confirm the presence of the **14**·Na complex, we attempted to get single crystals suitable for X-ray diffraction analysis. A single crystal of [**14**·Na]$^+$ was obtained by the crystallization from a mixture of free ligand **14** and $NaClO_4$ in methanol and the molecular structure of the complex is shown in Fig 3.[17] The metal ion is coordinated by the four nitrogen atoms of the tetraazamacrocyclic core and the three carbonyl oxygen atoms provided by the ester side arms. The Na-O and Na-N bond distances spanning in the range of 2.382(4) - 2.460(5) and 2.421(6) - 2.641(5) Å, respectively, are comparable with those previously reported for an analogous Na^+ complex derived from a cyclen derivative.[18]

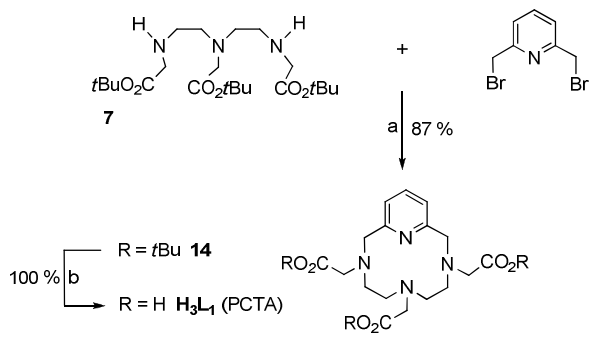

Scheme 4. Synthesis of ligand $\mathbf{H_3L_1}$ (PCTA). Reagents and conditions: (a) [reagents] = 2×10^{-3} M, Na_2CO_3, CH_3CN, reflux, 48 h; (b) aqueous 6*N* HCl, reflux, 12 h.

10.1002/ejoc.201800066

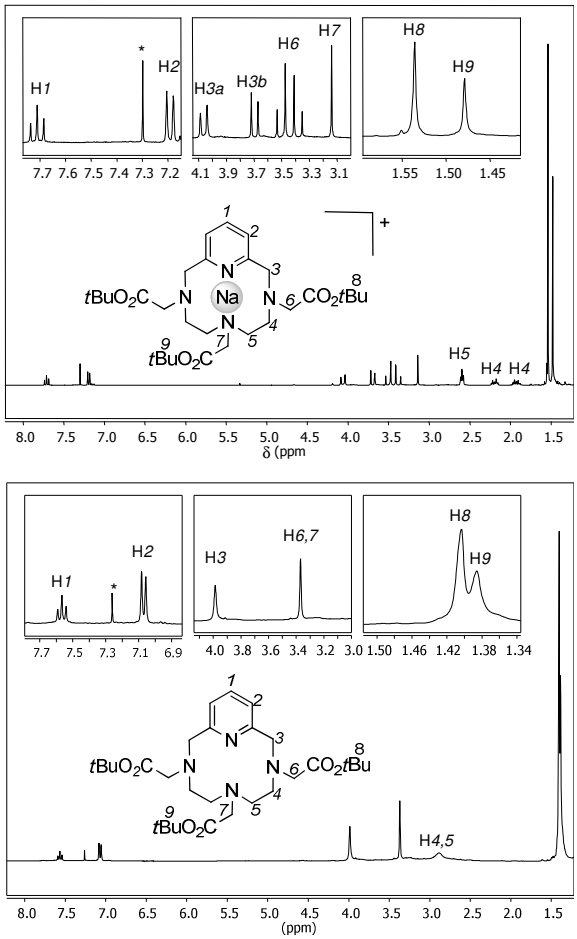

Figure 2. ^{1}H NMR spectra of **14** and **14**·Na in $CDCl_3$ at 300 MHz (* = solvent peak)

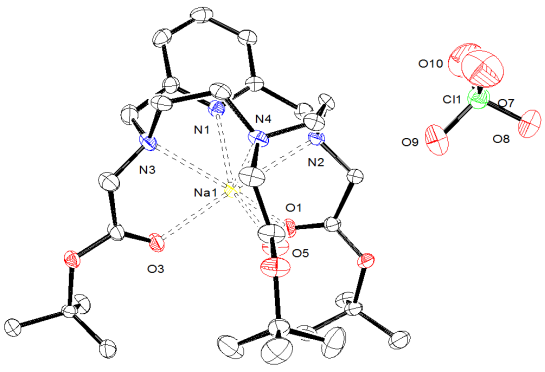

Figure 3. Complex [**14**·Na]ClO_4 structure. All hydrogen atoms were omitted for clarity.

The role of the respective nature of the leaving groups and of the base was then examined for the ring closure step by using the same experimental conditions (Table 2). A change in the

leaving group has a marked effect upon the yields of the macrocyclization reaction (entries 1, 3, 4). Tosylate and chloride gave product of comparable purity but in lower yields. The role of the nature of the base was examined during nucleophilic displacement of the bromide for the ring closure. The replacement of sodium carbonate by the organic base DIPEA does not inhibit the macrocyclization reaction as one might expect in the case of a metal ion template effect but decreased the yield of **14** to 53% (entries 1, 5). The difference in yields between 53 and 87%, whereas regarded as rather moderate, may reflect a template effect of the sodium cation. Changing the counter-cation of the inorganic base also affected intramolecular cyclization (entries 1, 6-8). In acetonitrile, sodium carbonate was the best catalyst followed by lithium, potassium and cesium carbonates, which gave decreasing yields of the 12-membered ring. We can note that the so-called "cesium effect" which has been found to be beneficial in Richman-Atkins cyclisation did not operate here.[19] In these reactions, no detectable 2:2 cyclization product was observed by MS analyses of the crude reaction mixture.

Table 2. Screening of leaving groups and bases in the macrocyclisation reaction[a]

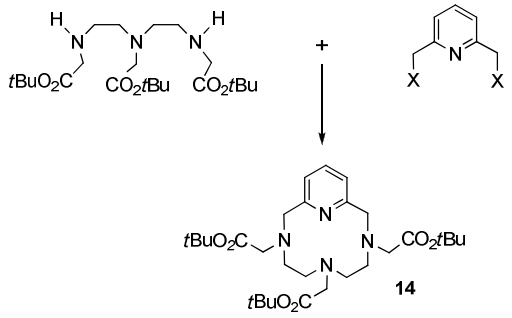

Entry	X	Base	**14** (isolated yields %)
1	Br	Na_2CO_3	87
2[b]	Br	Na_2CO_3	77
3	Cl	Na_2CO_3	35
4	OTs	Na_2CO_3	56
5	Br	DIPEA	53
6	Br	Li_2CO_3	59
7	Br	K_2CO_3	48
8	Br	Cs_2CO_3	26

[a] Reactions conditions: [reactants] = 2×10^{-3} M, base 1 equiv, CH_3CN, reflux, 48 h. [b] Reaction under microwave irradiation.

Finally, subsequent hydrolysis under acid conditions (aqueous 6*N* HCl) of the *tert*-butyl functions of **14** afforded $\mathbf{H_3L_1}$ (PCTA) as its tetra hydrochloride salt in a quantitative yield.

By using this approach, our currently obtained better macrocyclization yield (87%) can be favourably compared with those previously reported for the macrocyclization step leading to *N*,*N*′,*N*″-arylsulfonamide Pyclen derivative (~ 70%).[13] Moreover PCTA can be obtained in a better overall yield (60-65%) starting from diethylenetriamine or *N*-benzyl ethanol amine.

As a first illustration of this approach, we investigated the preparation of a PCTA platform derived from a 4-hydroxy pyridine moiety. The synthesis of this compound (**L_2**) starting from chelidamic acid is depicted in Scheme 5.

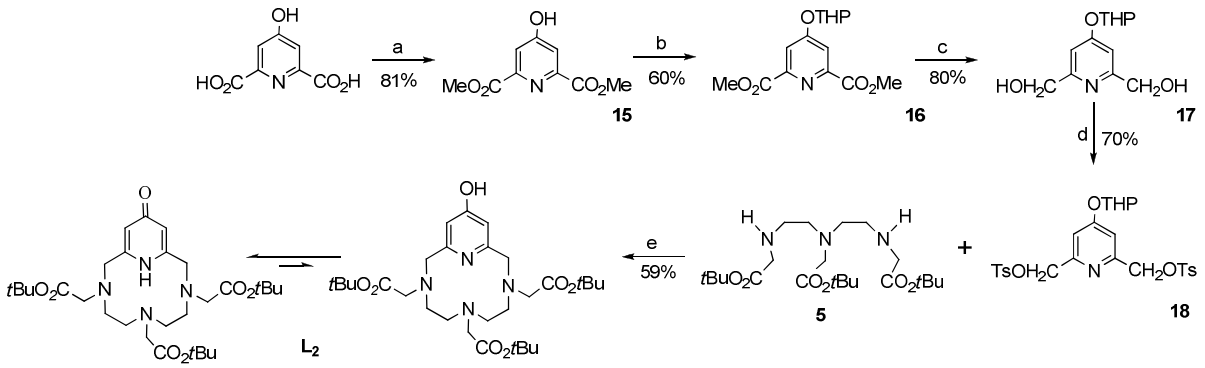

Scheme 5. Synthesis of ligand **L_2**. Reagents and conditions: (a) $SOCl_2$, MeOH, reflux, 6h (b) 3,4-dihydro-2*H*pyran, pyridinium *p*-toluenesulfonate, CH_2Cl_2, rt, 16h then 50 °C, 4h. (c) $NaBH_4$, $CaCl_2$, EtOH, 0 °C, 2h then rt, 1h. (d) TsCl, KOHaq, CH_2Cl_2, rt 16h. (e) compound **7**, Na_2CO_3, CH_3CN, reflux, 24h.

Esterification of chelidamic acid provided dimethylester **15** which upon protection of the hydroxyl group with dihydropyran (DHP) gave the protected diester **16**. Although $NaBH_4$ was effective for reducing this diester, a mixture of $NaBH_4$ and $CaCl_2$ produced diol **17** in a better yield (80 vs. 60 %). Our trials for conversion of alcohol groups of **17** to bromo groups in neutral conditions (NBS / PPh_3 system) were not successful. Hence we turned our efforts to the use of the corresponding bis sulfonate ester derivative **18** for the macrocyclization step. Intermolecular cyclization of triamine **5** and ditosylate **18** was accomplished under batchwise procedure and in the presence of Na_2CO_3, as described for **14**. After working up under mild acidic conditions and purification by column chromatography on alumina, free ligand **L_2** was obtained in 59 % yield. This result is in line with that observed for macrocycle **14** using tosylate as a leaving group (Table 2, entry 4). In comparison, Lincoln *et al.* reported the synthesis of a pyridol-based Pyclen in a three step-sequence and in analogous overall yield, starting from nosylated diethylenetriamine and a benzyl protected 4-pyridol derivative.[20] The

10.1002/ejoc.201800066

presence of the pyridone tautomer in chloroform was assessed by NMR analyses. The ^{1}H NMR spectrum displays a singlet at 6.07 ppm, characteristic of two aromatic protons in a pyridone ring and the ^{13}C NMR spectrum displays a signal at 180 ppm, attributed to C_4 atom of the pyridine ring and indicative of a carbonyl function.[21]

Then, we investigated the flexibility of this synthetic approach, studying the possibility to mix the nature of coordinating functions. In this further goal, we planned the access to PCTA[12] derivatives where amide and phosphinate functions are substituted for the carboxylic acid function in the central side arm (**H_3L_3** and **H_2L_4**, scheme 6).

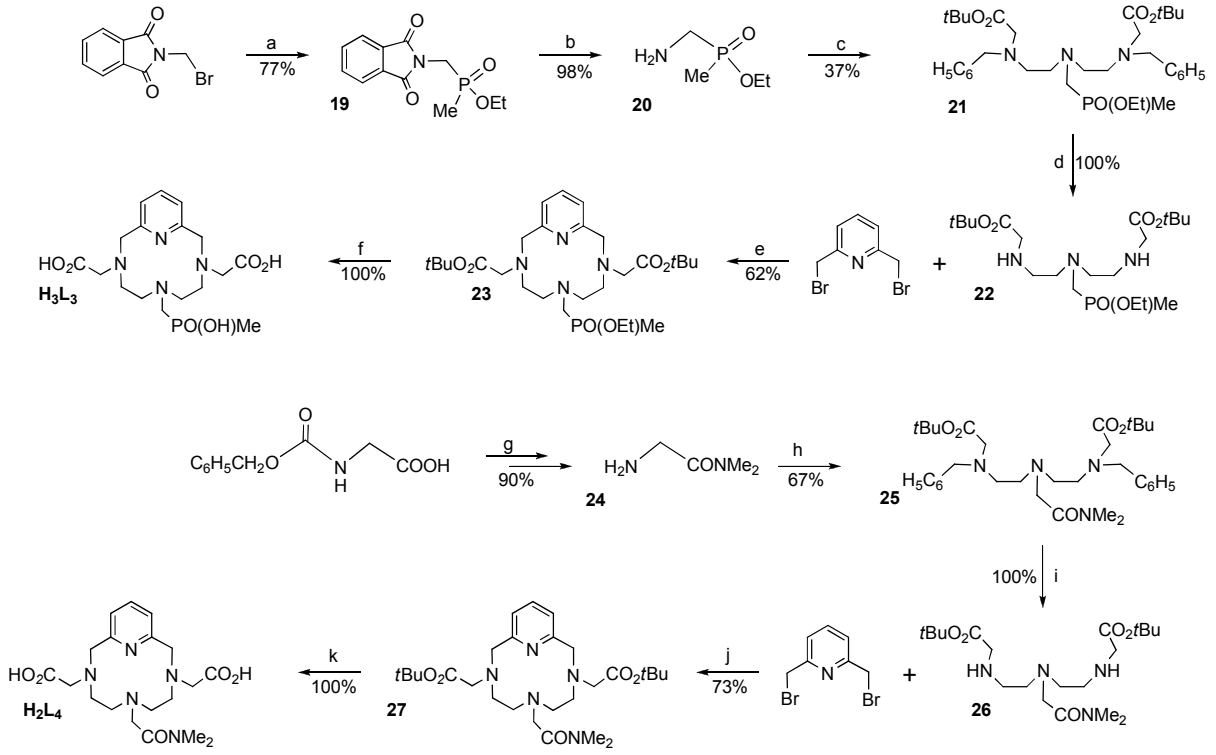

Scheme 6. Synthesis of ligand **H_3L_3** and **H_2L_4**. Reagents and conditions: (a) diethyl methylphosphonite, xylene, 300 mBar, 80 °C, 2h. (b) Hydrazine, EtOH, rt, 16h. (c) compound **5**, K_2CO_3, CH_3CN, reflux, 24h. (d) Pd/C (10%), H_2 gas (6 bars), MeOH, rt, 12h. (e) Na_2CO_3, CH_3CN, reflux, 48h. (f) aqueous 6*N* HCl, reflux, 12 h. (g) according to[25], (i) $Me_2NH.HCl$, EDCI, HOBt, DIPEA, DMF, rt, 16h, (ii) Pd/C (10%), H_2 gas , MeOH, rt, 16h. (h) compound **5**, K_2CO_3, CH_3CN, reflux, 24h. (i) Pd/C (10%), H_2 gas (6 bars), MeOH, rt, 12h. (j) Na_2CO_3, CH_3CN, reflux, 48h. (k) aqueous 6*N* HCl, reflux, 12 h.

The replacement of one acetic arm of polyaminocarboxylic macrocyclic ligands by methyleneamide or phosphinate groups has often been achieved and investigated.[22,23] This substitution may clearly influence several properties of the corresponding metallic complexes

such as thermodynamic stability, kinetic stability by hindering the access to the coordination sites of the metal ion, as well as overall electric charge of the complex, hydration number and lipophilicity. Amide and phosphinate groups can also act as starting points for the access of bifunctional chelates (BFCs) in the context of biomaterials or nanoparticles derivatization.[24]
The synthetic pathway for ligands **H_3L_3** and **H_2L_4** requires two starting materials, ethyl(aminomethyl)(methyl) phosphinate **20** and glycinedimethylamide **24** (Scheme 6). Amine **20** was prepared in a two-step procedure. According to the method of Popoff *et al.*, diethyl methylphosphonite and bromomethyl phtalimide were mixed in xylene and heated at 80°C for 2 h under reduced pressure (300 mBar).[25] In these conditions, the ethyl bromide that generated during the reaction was removed and **19** was obtained in 77% yield after column chromatography. Subsequent deprotection of the amine function was realized in the presence of hydrazine in ethanol. Varying both the quantity of hydrazine and time reaction leads to an optimal value of 1.7 equivalents of hydrazine and a 5 h heating at reflux for which only trace of starting materials remained. Glycinedimethylamide was also prepared in two steps from the Z-protected amino acid glycine by following the procedure of Guan *et al.*.[26]
Triamines **22** and **26** were then obtained upon bisalkylation of amine precursors **20** and **24** with 2 equiv of bromoderivative **5** in refluxing acetonitrile and in the presence of K_2CO_3 as base, followed by debenzylation of intermediates by catalytic hydrogenation. Condensation of triamines **22** and **26** with 2,6-dibromomethyl pyridine afforded the targeted free macrocycles **23** and **27** in 62 and 73 % yields, respectively. As previously observed for **14** and **L_2**, these macrocyclization reactions were controlled by a sodium template effect. Subsequent acid hydrolysis of *tert*-butyl ester and phosphinate ester functionalities afforded **H_3L_3** and **H_2L_4** as their hydrochloride salts in quantitative yields.

To test the effectiveness of ligands **H_3L_3** and **H_2L_4** to act as luminophores or paramagnetic contrast agents, their Ln(III) complexes (Ln = Eu, Tb, Gd) were prepared by mixing a slight excess of $LnCl_3$ salts and ligands in aqueous solution. The purity of the isolated complexes was checked by UPLC analysis and their structure determined by HRMS spectrometry. Interestingly, the Ln(III) complexes showed identical UPLC retention times within their respective series (**H_3L_3** and **H_2L_4**), suggesting that the lanthanide ions share the same coordination sphere for each complex series. Some luminescence and relaxometry properties in aqueous solution of these **L_3**·Ln and **L_4**·Ln complexes are gathered in table 3 and table 4.

10.1002/ejoc.201800066

Table 3. Photophysical data of Eu(III) and Tb(III) complexes derived from **H_3L_1**(PCTA), **H_3L_3** and **H_2L_4** ligands in aerated Tris-buffer (pH 7.4) at 298 K

	λ_{max} (nm)	ε (M^{-1} cm^{-1})	$I\,^7F_2$ / $I\,^7F_1$[a]	τ_{H2O} (ms)	τ_{D2O} (ms)	q_{H2O}[b]
L_1·Eu	270	3900	2.34	0.37	2.08	2.12
L_1·Tb	270	4100	-	1.24	2.91	2.02
L_1·Gd	270	4200	-	-	-	-
L_3·Eu	269	3600	2.49	0.38	2.06	2.04
L_3·Tb	269	3700	-	1.25	3.09	2.08
L_3·Gd	269	3600	-	-	-	-
L_4·Eu	270	3800	2.44	0.42	2.03	1.75
L_4·Tb	270	4000	-	1.31	3.12	1.91
L_4·Gd	270	3700	-	-	-	-

[a] integrated intensity ratio of $^5D_0 \rightarrow {}^7F_2$ and $^5D_0 \rightarrow {}^7F_1$ transitions. [b] Number of metal coordinated water molecules at 298K, calculated using the following equations: $q_{H2O}(Eu) = 1.11[(\tau_{H2O})^{-1} - (\tau_{D2O})^{-1} - 0.31]$[28c] and $q_{H2O}(Tb) = 5[(\tau_{H2O})^{-1} - (\tau_{D2O})^{-1} - 0.06]$[28b] with τ in ms.

Table 4. Relaxometric data at 20 MHz of Gd(III) complexes derived from **H_3L_1**(PCTA), **H_3L_3** and **H_2L_4** ligands in water at 20 MHz

	r_1^{298K} (s^{-1} mM^{-1})	r_1^{310K} (s^{-1} mM^{-1})	r_2^{310K} (s^{-1} mM^{-1})
L_1·Gd	6.9	5.4	6.3
L_3·Gd	8.2	5.8	7.2
L_4·Gd	7.1	5.5	5.9

Upon excitation to the absorption band of ligands (λ_{exc} = 270 nm), all Eu(III) and Tb(III) complexes exhibited the narrow characteristic red and green luminescence due to $^5D_0 \rightarrow {}^7F_J$ (J = 0-4) and $^5D_4 \rightarrow {}^7F_J$ (J = 3-6) transitions, respectively. In both cases, the hypersensitive $^5D_0 \rightarrow {}^7F_2$ transition at 615 nm and the sensitive $^5D_4 \rightarrow {}^7F_5$ transition at 545 nm are the most prominent (Figure 4). Due to the generally higher sensitivity of europium bands with regards to the coordination environment, the ratio between the intensity of the $^5D_0 \rightarrow {}^7F_2$ transition (electric dipole) and the intensity of the $^5D_0 \rightarrow {}^7F_1$ transition (magnetic dipole) gave valuable information about environment changes around the Eu(III) ion.[27] In comparison with PCTA·Eu complex, no major changes in the value of this ratio were observed in **L_3**·Eu and **L_4**·Eu chelates. This implies that the symmetry around the Eu(III) ion, both induced by the ligands and the solvent, is nearly constant. The temporal decays of the emission of both complexes were rigorously monoexponential showing the presence of a single emissive

solution species. At room temperature, the emission lifetimes are in the millisecond range compatible with the use of time resolved luminescence technique. These values are comparable to those of the parent PCTA[12] complexes. Owing to the well-established contribution of OH and OD oscillators to non-radiative decay rate and as well reported in the literature, comparison of lifetimes in deuterated and non deuterated water allowed us to determine quantitatively the q value (which provides the number of metal-bound water molecules) of these complexes.[28] This analysis indicated that two water molecules are present in the first coordination sphere of the metal in both complexes. These data clearly indicate that these new chelates did not limit the accessibility of water molecules to the lanthanide ion, in spite of the steric hindrance of amide and phosphinate groups. In addition, the overall emission quantum yields were determined by excitation of the ligands (λ_{exc} = 270 nm) and are similar to those of PCTA complexes (Φ^L(Eu) = 3 %, Φ^L(Tb) = 8 %). These results are not unexpected due to the same inner-sphere hydration (q = 2) and the same antenna unit in these three complexes.

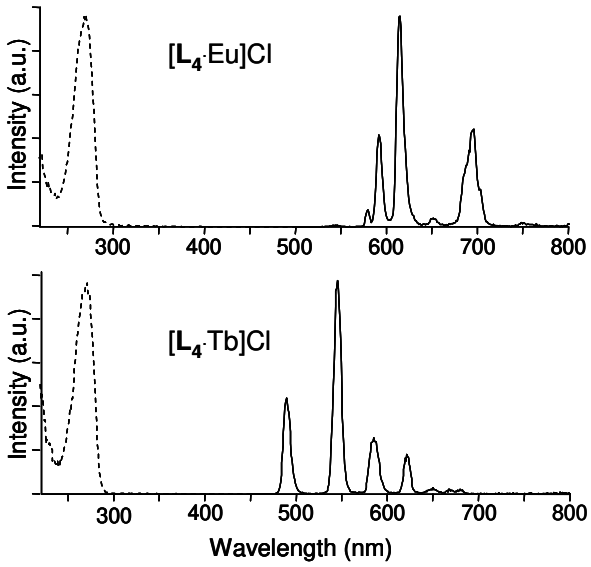

Figure 4. Normalized excitation (- - -) and luminescence (——) spectra of [**L$_4$**·Eu]Cl and [**L$_4$**·Tb]Cl complexes. These spectra were measured at 298 K in Tris buffer (pH 7.4).

The relaxometric properties of **L$_3$**·Gd and **L$_4$**·Gd were assessed by measuring their overall relaxivity r_1 which represents the increase in the longitudinal nuclear magnetic relaxation rate of water protons promoted by the paramagnetic complex. At 20 MHz and 310 K, the r_1 values of **L$_3$**·Gd (5.8 s^{-1} mM^{-1}) and **L$_4$**·Gd (5.5 s^{-1} mM^{-1}) are larger than those found in mono-aqua

contrast agent DTPA·Gd (3.8 s^{-1} mM^{-1}) and DOTA·Gd (3.5 s^{-1} mM^{-1}) which are currently used in clinical practice.[29] They are similar to that of PCTA·Gd and in the range of those reported for bis-hydrated Gd(III) complexes of small size and with no self-aggregation properties.[30] It is also interesting to note that relaxivity r_1 of **L_3**·Gd at 298 K (8.2 s^{-1} mM^{-1}) is close to that reported for PCP2A·Gd (r_1^{298K} = 8.3 s^{-1} mM^{-1} at 20 MHz), where phosphonate function is substituted for the phosphinate function in the central arm.[31] These relaxometric data confirm the number of hydration q = 2 established by luminescence experiments of the corresponding Eu(III) and Tb(III) complexes. The temperature dependence of relaxivity r_1 at 20 MHz for the two complexes was also measured in the range 278 – 318 K and is reported in Figure 5. Analogous data for PCTA·Gd complex is also shown for comparison. For the two complexes, relaxivity r_1 increases with decreasing temperature, revealing that the exchange between the coordinated water molecules and bulk water (τ_M) does not limit the relaxation rate. On the other hand when the relaxivity is limited by the water exchange, either a plateau or a decrease of the relaxivity is observed at low temperature.[32] Further work should be undertaken about the evaluation of τ_M by oxygen-17 relaxometry, as well as inertness of these neutral and cationic Gd^{III} complexes towards di-anions present in human plasma such as carbonate. Actually, the two inner-sphere water molecules of bis-hydrated Gd^{III} complexes may be displaced by di-anions leading to ternary adducts of lower hydration state and thus lower relaxivity, as reported in the literature.[5,33]

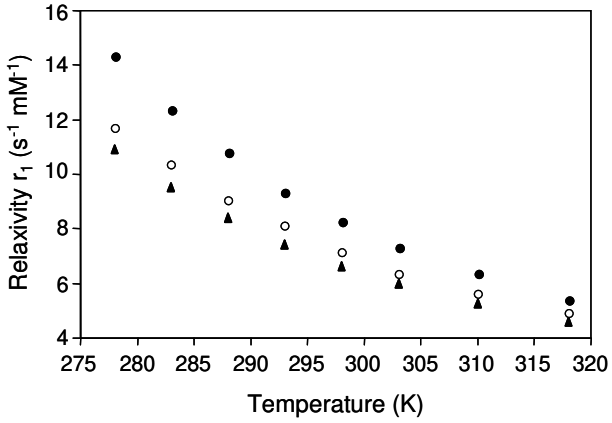

Figure 5. Temperature (278 – 318 K) dependence of the proton longitudinal relaxivity, r_1, of **L_1**·Gd (closed triangles, c = 0.536 mM), **L_3**·Gd (closed circles, c = 0.262 mM) and [**L_4**·Gd]Cl (open circles, c = 1.713 mM) complexes in water at 20 MHz.

Conclusions

In conclusion, we describe a convenient synthetic pathway for the access of the 12-membered PCTA macrocycle, whose metallic complexes possess a number of favourable properties in the fields of biomedical imaging and radiotherapy. This procedure appears as an efficient alternative compared to the nowadays preparation of PCTA[12] and its derivatives based on the classical Richman-Atkins methodology. In addition, we demonstrate that such an approach is general and can be successfully applied to PCTA derivatives containing either substituted pyridine unit or mixed coordinating functions. Moreover, we reported the luminescence and relaxometry properties of Ln(III) complexes of the two novel PCTA[12] derivatives bearing amide or phosphinate functions in the central side arm. The photophysical studies established that the Eu(III) and Tb(III) complexes are bis-hydrated and do not impair the luminescence characteristics of PCTA europium and terbium complexes. The relaxometric experiments on Gd(III) complexes confirm an enhanced relaxivity associated with the presence of two coordinated water molecules and indicate that the relaxivity is not limited by the water exchange rate but rather by the fast rotational motion of these low molecular weight Gd-chelates. Finally, we believe that this synthetic pathway may open up a new way for the synthesis of other PCTA[12] derivatives, especially bifunctional chelates (BFCs) suitable for conjugation and applications

Experimental Section

For table of abbreviations, information concerning details of the experimental procedure and characterization of compounds **4**-**12, 14** and $\mathbf{H_3L_1}$, **15**-**18** and $\mathbf{L_2}$, **19**-**23 and** $\mathbf{H_3L_3}$ and **24**- **27** and $\mathbf{L_2H_4}$; selected bond lengths and angles for [**14**·Na]ClO_4 complex; ^{1}H, ^{13}C NMR and MS spectra of selected compounds; UPLC chromatograms and HRMS spectra of Ln(III) complexes; luminescence emission spectra of Eu(III) complexes, please use our Supporting Information.

Acknowledgements

This work was financially supported by the French Ministère de la Recherche (Ph.D. grant for E M), the Centre National de la Recherche Scientifique (CNRS) and the Cancéropôle Grand-Sud Ouest. We thank Dr Isabelle Nasso for preliminary work on the synthesis of PCTA[12],

Isabelle Fabing for technical assistance on UPLC equipment provided by the Integrated Screening Platform of Toulouse (PICT, IBiSA), Dr Rémy Brousses for X-ray diffraction study and Pr Luce Vander Elst, Dr Sophie Laurent (University of Mons, Belgium) for assistance in relaxometric measurements.

---

[1] For selected recent reviews, see: a) E. W. Price, C. Orvig, *Chem. Soc. Rev.* **2014**, *43*, 260-290; b) G. J. Stasiuk, N. J. Long, *Chem. Commun.* **2013**, *49*, 2732-2746.

[2] H. Stetter, W. Frank, R. Mertens, *Tetrahedron* **1981**, *37*, 767-772.

[3] G. Tircso, E. T. Benyo, E. H. Suh, P. Jurek, G. E. Kiefer, A. D. Sherry, Z. Kovacs, *Bioconjugate Chem.* **2009**, *20*, 565-575.

[4] a) W. D. Kim, G. E. Kiefer, F. Maton, K. Mcmillan, R. N. Muller, A. D. Sherry, *Inorg. Chem.* **1995**, *34*, 2233-2243; b) G. Bort, S. Catoen, H. Borderies, A. Kebsi, S. Ballet, G. Louin, M. Port, C. Ferroud, *Eur. J. Med. Chem.* **2014**, *87*, 843-861.

[5] M. Port, I. Raynal, L. Vander Elst, R. N. Muller, F. Dioury, C. Ferroud, A. Guy, *Contrast Med. Mol. Imaging* **2006**, *1*, 121-127.

[6] a) J.-M. Siaugue, F. Segat-Dioury, A. Favre-Reguillon, V. Wintgens, C. Madic, J. Foos, A. Guy, *J. Photochem. Photobiol. A* **2003**, *156*, 23-29; b) M. Enel, N. Leygue, S. Balayssac, S. Laurent, C. Galaup, L. Vander Elst, C. Picard, *Dalton Trans.* **2017**, *46*, 4654-4668.

[7] a) C. L. Ferreira, D. T. Yapp, E. Lamsa, M. Gleave, C. Bensimon, P. Jurek, G. E. Kiefer, *Nucl. Med. Biol.* **2008**, *35*, 875-882; b) C. L. Ferreira, E. Lamsa, M. Woods, Y. Duan, P. Fernando, C. Bensimon, M. Kordos, K. Guenther, P. Jurek, G. E. Kiefer, *Bioconjugate Chem.* **2010**, *21*, 531-536; c) C. L. Ferreira, D. T. T. Yapp, D. Mandel, R. K. Gill, E. Boros, M. Q. Wong, P. Jurek, G. E. Kiefer, *Bioconjugate Chem.* **2012**, *23*, 2239-2246.

[8] a) C. L. Ferreira, I. Holley, C. Bensimon, P. Jurek, G. E. Kiefer, *Mol. Pharmaceutics* **2012**, *9*, 2180-2186; b) H. Zolata, F. Abbasi Davani, H. Afarideh, *Nucl. Med. Biol.* **2015**, *42*, 164-170.

[9] a) R. Chakravarty, S. Chakraborty, A. Dash, *J. Label Compd. Radiopharm* **2014**, *57*, 65-74; b) U. Pandey, N. Gamre, Y. Kumar, P. Shetty, H. D. Sarma, A. Dash, *J. Radioanal. Nucl. Chem.* **2016**, *307*, 187-194; c) M. Le Fur, M. Beyler, N. Lepareur, O. Fougère, C. Platas-Iglesias, O. Rousseaux, R. L. Tripier, *Inorg. Chem.* **2016**, *55*, 8003-8012.

[10] J. E. Richman, T. J. Atkins, *J. Am. Chem. Soc.* **1974**, *96*, 2268-2270.

[11] a) G. Bechara, N. Leygue, C. Galaup, B. Mestre-Voegtlé, C. Picard, *Tetrahedron* **2010**, *66*, 8594-8604; b) I. Nasso, C. Galaup, F. Havas, P. Tisnès, C. Picard, S. Laurent, L. Vander Elst, R. N. Muller, *Inorg. Chem.* **2005**, *44*, 8293-8305.

[12] V. Marti-Centelles, M. D. Pandey, M. I. Burguete, S. V. Luis, *Chem. Rev.* **2015**, *115*, 8736-8834.

[13] a) S. Aime, M. Botta, S. Geninatti Crich, G. B. Giovenzana, G. Jommi, R. Pagliarin, M. Sisti, *Inorg. Chem.* **1997**, *36*, 2992-3000; b) J.-M. Siaugue, F. Segat-Dioury, A. Favre-Reguillon, C. Madic, J. Foos, A. Guy, *Tetrahedron Lett.* **2000**, *41*, 7443-7446.

[14] C. Galaup, J.-M. Couchet, S. Bedel, P. Tisnès, C. Picard, *J. Org. Chem.* **2005**, *70*, 2274-2284.

[15] E. W. Price, J. F. Cawthray, G. A. Bailey, C. L. Ferreira, E. Boros, M. J. Adam, C. Orvig, *J. Am. Chem. Soc.* **2012**, *134*, 8670-8683.

[16] H.-S. Chong, X. Ma, H. Lee, P. Bui, H. A. Song, N. Birch, *J. Med. Chem.* **2008**, *51*, 2208-2215.

[17] CCDC-1590053 contains the supplementary crystallographic data for this paper. These data can be obtained free of charge from the Cambridge Crystallographic Data Centre.

[18] T. Koullourou, L. S. Natrajan, H. Bhavsar, S. J. A. Pope, J. Feng, J. Narvainen, R. Shaw, E. Scales, R. Kauppinen, A. M. Kenwright, S. Faulkner, *J. Am. Chem. Soc.* **2008**, *130*, 2178-2179.

[19] A. Ostrowicki, E. Koepp, F Vögtle, *Topics in Current Chemistry: Macrocycles*, Vol. 161; Springer-Verlag, 1992, p. 37.

[20] K. M. Lincoln, P. Gonzalez, T. E. Richardson, D. A. Julovich, R. Saunders, J. W. Simpkins, K. N. Green, *Chem. Commun.* **2013**, *49*, 2712-2714.

[21] a) J. S. Bradshaw, P. Huszthy, H. Koyama, S. G. Wood, S. A. Strobel, R. B. Davidson, R. M. Izatt, N. K. Dalley, J. D. Lamb, J. J. Christensen, *J. Heterocyclic Chem.* **1986**, *23*, 1837-1843; b) C. J. Turner, G. W. H. Cheeseman, *Org. Magn. Resonance* **1974**, ***6***, 663-666.

[22] a) E. J. Shiells, L. S. Natrajan, D. Sykes, M. Tropiano, P. Cooper, A. M. Kenwright, S. Faulkner, *Dalton Trans.* **2011**, *40*, 11451-11457; b) L. Tei, G. Gugliotta, Z. Baranyai, M. Botta, *Dalton Trans.* **2009**, 9712-9714; c) D. Thonon, V. Jacques, J. F. Desreux, *Contrast Media Mol. Imaging* **2007**, *2*, 24-34.

[23] a) R. Kerdjoudj, M. Pniok, C. Alliot, V. Kubicek, J. Havlickova, F. Rosch, P. Hermann, S. Huclier-Markai, *Dalton Trans.* **2016**, *45*, 1398-1409; b) G. Máté, J. Šimecek, M. Pniok, I. Kertész, J. Notni, H.-J. Wester, L. Galuska, P. Hermann, *Molecules* **2015**, *20*, 13112-13126.

[24] a) S. N. M. Chilla, O. Zemek, J. Kotek, S. Boutry, L. Larbanoix, C. Sclavons, L. V. Elst, I. Lukes, R. N. Muller, S. Laurent, *Bioorg. Med. Chem.* **2017**, *25*, 4297-4303; b) A. F. Martins, D. M. Dias, J.-F. Morfin, S. Lacerda, D. V. Laurents, E. Toth, C. F. G. C. Geraldes, *Chem. Eur. J* **2015**, *21*, 5413-5422; c) P. Rezanka, V. Kubícek, P. Hermann, I. Lukeš, *Synthesis* **2008**, 1431-1435.

[25] I. C. Popoff, L. K. Huber, B. P. Block, P. D. Morton, R. P. Riordan, *J. Org. Chem.* **1963**, *28*, 2898-2900.

[26] M. Guan, Y. Pang, J. Zhang, Y. Zhao, *Chem. Commun.* **2016**, *52*, 7043-7046.

[27] K. Binnemans, *Coord. Chem. Rev.* **2015**, *295*, 1-45.

[28] a) W. D. Horrocks, D. R. Sudnick, *Acc. Chem. Res.* **1981**, *14*, 384-392; b) A. Beeby, I. M. Clarkson, R. S. Dickins, S. Faulkner, D. Parker, L. Royle, A. S. De Sousa, J. A. G. Williams, M. Woods, *J. Chem. Soc., Perkin Trans. 2* **1999**, 493-503; c) R. M. Supkowski, W. D. W. Horrocks Jr., *Inorg. Chim. Acta* **2002**, *340*, 44-48.

[29] S. Laurent, L. Vander Elst, R. N. Muller, *Contrast Med. Mol. Imaging* **2006**, *1*, 128–137.

[30] a) C. S. Bonnet, S. Laine, F. Buron, G. Tircso, A. Pallier, L. Helm, F. Suzenet, E. Toth, *Inorg. Chem.* **2015**, *54*, 5991-6003; b) E. M. Gale, N. Kenton, P. Caravan, *Chem. Commun.* **2013**, *49*, 8060-8062; c) Z. Baranyai, L. Tei, G. B. Giovenzana, F. K. Kalman, M. Botta, *Inorg. Chem.* **2012**, *51*, 2597-2607.

[31] S. Aime, M. Botta, L. Frullano, S. Geninatti Crich, G. Giovenzana, R. Pagliarin, G. Palmisano, F. R. Sirtori, M. Sisti, *J. Med. Chem.* **2000**, *43*, 4017-4024.

[32] S. Laurent, F. Botteman, L. Vander Elst, R. N. Muller, *Eur. J. Inorg. Chem.* **2004**, 463-468.

[33] a) E. Boros, P. Caravan, *Inorg. Chem.* **2015**, *54*, 2403-2410; R. Negri, Z. Baranyai, L. Tei, G. B. Giovenzana, C. Platas-Iglesias, A. C. Bényei, J. Bodnar, A. Vagner, M. Botta, *Inorg. Chem.* **2014**, *53*, 12499-12511; c) D. Imperio, G. B. Giovenzana, G.-L. Law, D. Parker, J. W. Waltona, *Dalton Trans.* **2010**, *39*, 9897–9903.

10.1002/ejoc.201800066

Table of contents entry

Facile access to 12-membered macrocyclic ligand PCTA and novel derivatives including carboxylate, amide and phosphinate ligating functionalities.

Morgane Enel, Nadine Leygue, Nathalie Saffon, Chantal Galaup, and Claude Picard

Macrocyclic ligands, lanthanides

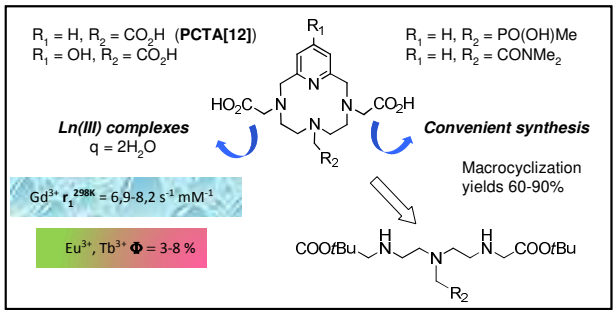

A convenient and efficient alternative to the classical Richman-Atkins methodology for obtaining PCTA[12] and new derivatives is reported. The key macrocyclization step occurs in good yields as a result of a sodium template effect. The potentiality of lanthanide (III) complexes derived from these new PCTA[12] ligands to act as paramagnetic contrastophores or luminophores is reported.